PERGAMON

International Journal of Solids and Structures 38 (2001) 7487–7500

INTERNATIONAL JOURNAL OF SOLIDS and STRUCTURES

www.elsevier.com/locate/ijsolstr

# An improved energy criterion for dynamic buckling of imperfection sensitive nonconservative systems

A.N. Kounadis [a,*], C.J. Gantes [a], V.V. Bolotin [b]

[a] *Department of Civil Engineering, Struct Analysis and Steel Bridges, National Technical University of Athens, 42 Patission Street, 10682 Athens, Greece*

[b] *Institute of Mechanical Engineering Research, Laboratory of Reliability, Russian Academy of Sciences, Russian Federation, M. Kharitonyevsky Lane, 101830 Moscow, Russia*

Received 22 May 2000

**Abstract**

Imperfection sensitive, multi-degree-of-freedom, autonomous, structural systems under partial follower compressive loading, which lose their stability via divergence are investigated both qualitatively and quantitatively. Attention is focused on the global instability of that equilibrium state on the locally stable primary path, which at a certain level of the loading becomes globally unstable. Previous work valid for potential systems under step loading is extended here to nonpotential, imperfection sensitive systems. The serious difficulty of the lack of potential of the follower type of loading is overcome by formulating an appropriate energy balance equation, including loss of energy. Then, similar considerations to those for potential systems can be established, and geometric criteria can be formulated for an "equivalent energy" surface. Using the mean-value theorem for integrals one can obtain approximate dynamic buckling loads that are very good for structural design purposes. The efficiency and reliability of the proposed method is comprehensively demonstrated through numerous examples. 

*Keywords:* Dynamic buckling; Nonconservative systems; Energy criterion; Imperfection sensitivity

## 1. Introduction

The recent developments in hydro and aeromechanics have increased substantially the interest of structural analysis in nonpotential (nonconservative), non-self-adjoint problems. The wind-induced collapse of Takoma Narrows Bridge, aerospace structures under follower forces produced by jet and rocket thrusts, problems of fluid–structure interaction, oscillations of pipes conveying fluids (Paidoussis, 1997) are interesting examples of engineering applications. Nonpotential systems under partial follower (i.e. path dependent) load may lose their stability either by divergence (static instability) or by flutter (dynamic instability). The static critical load is obtained via a classical analysis by applying either the static or the kinetic Ziegler's criterion, associated with the vanishing of the fundamental circular frequency, while the

* Corresponding author. Tel.: +30-1-772-3441; fax: +30-1-772-3442.
*E-mail address:* kounadis@central.ntua.gr (A.N. Kounadis).

0020-7683/01/$ - see front matter 
PII: S0020-7683(01)00042-7

dynamic (flutter) critical load is established only by employing the *dynamic* or *kinetic* criterion. A large amount of pertinent work has been published in the last thirty years (Bolotin, 1963; Huseyin, 1978; Inman, 1983; Kandakis and Kounadis, 1992; Kounadis, 1977, 1983, 1992; Leipholz, 1970; Moran, 1970; Walker and Schmitendorf, 1973; Ziegler, 1952).

Exact dynamic buckling loads (DBLs) of general discrete systems can be determined *only* through a *global* (nonlinear) dynamic analysis associated with several drawbacks mentioned above. Nevertheless, one can obtain practically "exact" DBLs via a suitable *geometric* approach, employed for *n*-degree of freedom (*n*-DOF) systems, which under *statically* applied load experience either a *limit point instability* (Fig. 1a) or an *unstable branching point* bifurcating from a *nonlinear prebuckling* path (Fig. 1b).

In a recent work (Kounadis, 1994a), it was shown that the loss of stability of a perfect bifurcational model of 2-DOF may occur via flutter (through a Hopf bifurcation) in regions of divergence instability; hence, the classical static stability analysis and Ziegler's kinetic criterion may fail to predict the actual critical load. In this region, it was also found that these systems may be associated with a double zero eigenvalue and exhibit one postbuckling path passing through the 1st and 2nd branching point. Very recently, Kounadis and Simitses (1997), have also shown that the above perfect bifurcational nonconservative systems may exhibit a limit cycle response, even in case they are associated with symmetrizable stiffness matrices, contrary to existing results (Inman, 1983; Leipholz, 1970).

The major part of the existing work refers mainly to perfect bifurcational nonconservative systems (with trivial fundamental equilibrium paths) and only a few studies deal with imperfection sensitive (or limit point) nonconservative systems (Kounadis, 1991; Kounadis et al., 1992; Plaut 1976). It was found numerically (Kounadis, 1991; Kounadis et al., 1992) that the actual critical load of imperfection sensitive nonconservative systems is not the limit point load but a lower load obtained only with the aid of a nonlinear *dynamic* analysis, in contrast with existing stability analyses (Plaut, 1976).

Despite the availability of high-speed computers and computational techniques, quite often one has to overcome numerical difficulties due to large time solutions (Kounadis, 1991, 1999), solutions very sensitive to initial conditions or to damping (Kounadis, 1991, 1999) or solutions associated with alternative narrow regions of stability and instability (Kounadis, 1995). Due to these difficulties numerical methods become time consuming, some times less reliable, and possibly erroneous, if correct solutions are missed. These drawbacks become more acute in case of multiple-parameter investigations.

The objective of this study is to present a qualitative dynamic buckling analysis of imperfection sensitive nonconservative systems under partial follower compressive loading, based on energy and geometrical considerations which for 2-DOF systems may lead to approximate but very reliable for structural design purposes DBLs without solving the highly nonlinear initial-value problem. New findings, as byproducts of this work, will be also reported.

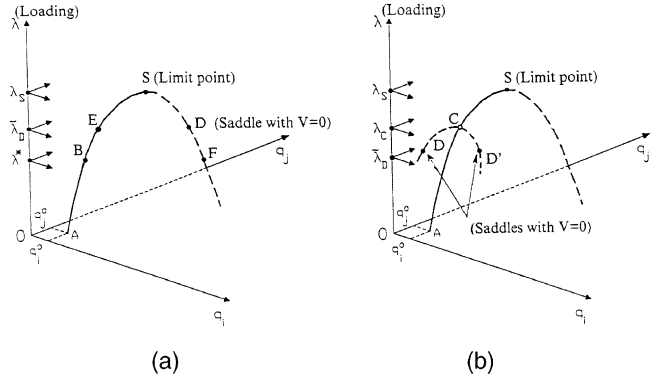


Fig. 1. Nonlinear equilibrium paths ($\lambda$ vs $q_i$ and $q_j$): (a) of a typical limit point system and (b) of an unstable bifurcational system.

## 2. Description of the problem

The dynamic response of a general $n$-DOF, $n$-mass, dissipative system under partial follower loading $\lambda$ associated with a nonconservativeness parameter $\eta$, is discussed below. Lagrange differential equations of motion for this autonomous nonpotential system in terms of generalized displacements $q_i$ and generalized velocities $\dot{q}_i$, are given by

$$\frac{\mathrm{d}}{\mathrm{d}t}\left(\frac{\partial K}{\partial \dot{q}_i}\right)-\frac{\partial K}{\partial q_i}+\frac{\partial F}{\partial \dot{q}_i}+\frac{\partial U}{\partial q_i}-Q_i=0,\quad i=1,\ldots,n \tag{1}$$

where the dots denote differentiation with respect to time $t$; $K=(1/2)a_{ij}\dot{q}_i\dot{q}_j$ is the positive definite function of the total kinetic energy with diagonal elements being functions of masses $m_i$ [i.e. $a_{ii}=a_{ii}(m_i)$, $i=1,\ldots,n$] and nondiagonal elements being functions of $m_i$ and $q_i$ [i.e. $a_{ij}=a_{ij}(m_i,q_i)$ for $i\neq j$, $i,\ j=1,\ldots,n$]; $F=(1/2)c_{ij}\dot{q}_i\dot{q}_j$ is a positive or nonnegative definite dissipation function with coefficients $c_{ij}=c_{ij}(c_i)$ which could also be functions of $q_i$ [i.e. $c_{ij}=c_{ij}(c_i;q_i)$ with $i,j=1,\ldots,n$], where $c_i$ are viscous damping coefficients; $U=U(q_i;k_i)$ is the positive definite function of the elastic strain energy, being a nonlinear function of $q_i$, while $k_i$ represent linear stiffness parameters (nonlinear spring components may also be included); $Q_i=\lambda\overline{Q}_i(q_i,q_i^0,\eta)$ are generalized nonpotential forces, being linear functions of $\lambda$ and nonlinear functions of $q_i$, $q_i^0$ (initial imperfections) and $\eta$. For a certain value of $\eta$, $\eta=\eta_0$, the external forces become conservative (potential), while for $\eta<\eta_0$ or $\eta>\eta_0$ (boundary between flutter and divergence) adjacent equilibria do not exist (Kounadis, 1994a). The static equilibrium and buckling equations are given by

$$\begin{aligned} &V_i=U_i-\lambda\overline{Q}_i=0,\quad i=1,\ldots,n\\ &\det[V_{ij}]=\det([U_{ij}])-\lambda[\overline{Q}_{ij}]=0 \end{aligned} \tag{2}$$

where $U_i=\partial U/\partial q_i$, while $[V_{ij}]$ and $[U_{ij}]=[\partial^2U/\partial q_i\partial q_j]$ are symmetric matrices, and $[\overline{Q}_{ij}]=[\partial\overline{Q}_i/\partial q_j]$ is a square nonsingular asymmetric matrix for $\eta\neq\eta_0$ (non-self-adjoint system). Note also that $[V_{ij}]=[\overline{Q}_{ij}]([\tilde{U}_{ij}]-\lambda I)$, where $[\tilde{U}_{ij}]=[\overline{Q}_{ij}]^{-1}[U_{ij}]$ is an asymmetric stiffness matrix, the eigenvalues of which are the static bifurcational buckling loads, while $I$ is the identity matrix.

For a system initially ($t=0$) unstressed under step loading we can assume the following initial conditions

$$q_i(0)=q_i^0,\quad \dot{q}_i(0)=0 \tag{3}$$

due to which

$$K|_{t=0}=U|_{t=0}=0 \tag{4}$$

The follower loading $\lambda$ and the nonconservativeness parameter $\eta$ are the main control parameters for static and dynamic bifurcations (Kounadis, 1994a,1995; Kounadis and Simitses, 1993) as well as for the stability of equilibria and limit cycles. Dynamic bifurcation is defined as a sudden *qualitative* change of the system response (occurring at a certain value of a smoothly varying control parameter) due to which the phase-portrait is changed to a topologically non-equivalent portrait.

## 3. Dynamic analysis

The lack of potential of systems under follower type loading constitutes a serious difficulty for establishing a qualitative dynamic buckling analysis similar to that holding for conservative (potential) loads (Kounadis, 1994b, 1996b, 1999). However, one can overcome this drawback via an energy-balance equation, as shown below.

Writing Eq. (1) for $i = 1, 2, \ldots, n$, thereafter multiplying these equations by $\dot{q}_1, \dot{q}_2, \ldots, \dot{q}_n$ respectively, subsequently integrating them with respect to time $t$, and summing up the resulting equations, we get the following energy-balance equation (including loss of energy)

$$K + 2\int_0^t F\mathrm{d}t' + U - \lambda \int_0^t \left(\sum_{i=1}^{n} \overline{Q}_i \dot{q}_i\right)\mathrm{d}t' = C \tag{5}$$

where $C = 0$ for a system initially $(t = 0)$ unstressed, due to Eq. (4). Hence, Eq. (5) can also be written as follows

$$K + 2\int_0^t F\mathrm{d}t' + V = 0 \tag{6}$$

where

$$V = U - \lambda \int_0^t \left(\sum_{i=1}^{n} \overline{Q}_i \dot{q}_i\right)\mathrm{d}t' \tag{7}$$

The integral of Eq. (7) is, in general, not integrable in terms of known functions. However, it can be approximated in various ways (e.g. by using the mean-value theorem for integrals). Nevertheless, the above integral is integrable in case of 1-DOF systems (Kounadis, 1996a). Clearly, condition (6) is similar to that valid for potential systems (Kounadis, 1994b, 1996a,b), but with $V$ which cannot be given in closed form, since the integral in Eq. (7) is not integrable. Since $K$ and $F$ are positive definite functions, Eq. (6) implies that throughout the motion $V < 0$.

Using the stability criterion of Laplace or Lagrange (boundedness of solution), valid for potential systems, dynamic buckling is defined as that state for which an escaped motion leads either to an unbounded motion (overflow) or to a large response associated with a remote stable equilibrium point (acting as attractor) if damping is included. The minimum load of this state is defined as the DBL $\lambda_{\mathrm{DD}}$ (if damping is included) or $\lambda_{\mathrm{D}}$ (if damping is neglected). For $\lambda < \lambda_{\mathrm{DD}}$ the motion is captured by the asymptotically stable equilibria of the fundamental (nonlinear) equilibrium path. The above definitions and phenomena hold also for nonpotential systems. Using a Taylor's expansion (Kounadis, 1994b, 1996a), it was established that $\lambda_{\mathrm{D}}$ has always as lower bound the load $\tilde{\lambda}_{\mathrm{D}}$ associated with vanishing but nonzero damping. However, numerical results show that *this is not true for nonpotential systems*, i.e. $\tilde{\lambda}_{\mathrm{D}}$ may be greater or lower than $\lambda_{\mathrm{D}}$. Nevertheless, using energy and geometrical considerations one can estimate a priori the degree of deviation of $\tilde{\lambda}_{\mathrm{D}}$ from $\lambda_{\mathrm{D}}$ for both potential (Kounadis, 1996b, 1999) and nonpotential systems (Kounadis, 1998). As will be shown below, such an energy criterion yielding $\tilde{\lambda}_{\mathrm{D}}$ can be further improved leading to a very accurate load $\overline{\lambda}_{\mathrm{D}}$.

The load $\tilde{\lambda}_{\mathrm{D}}$ and the corresponding *saddles* $q_i^{\mathrm{D}}$ (on the unstable path) are obtained for given initial conditions (3) by solving the systems of $(n + 1)$ equations

$$\left.\begin{array}{l} V_i(q_i, \lambda; q_i^0) = 0 \\ V_i(q_i, \lambda; q_i^0) = 0 \end{array}\right\} \quad i = 1, \ldots, n \tag{8}$$

For nonconservative systems, the error (difference) $E = \lambda_{\mathrm{D}} - \tilde{\lambda}_{\mathrm{D}}$ is more conveniently determined by considering 2-DOF systems for which one has a *geometric picture* of the total potential energy "surface" $V(q_i, \lambda; q_i^0)$ in the 3-D $V$-displacement space. For such a model at a fixed load $\overset{*}{\lambda} < \tilde{\lambda}_{\mathrm{D}}$ the "surface" $V(q_i, \lambda; q_i^0)$ passing through the point A (defined by the initial displacements $\varepsilon_1, \varepsilon_2$), the *stable* equilibrium B (defined by $q_1^{\mathrm{B}}, q_2^{\mathrm{B}}$) and the *saddle* F (defined by $q_1^{\mathrm{B}}, q_2^{\mathrm{B}}$) is shown in Fig. 2a. Points B and F correspond both to $\overset{*}{\lambda}$. At point B the total potential $V$ is *minimum*, at point A we have $V = 0$, while $V$ at the *saddle* F is *positive*.

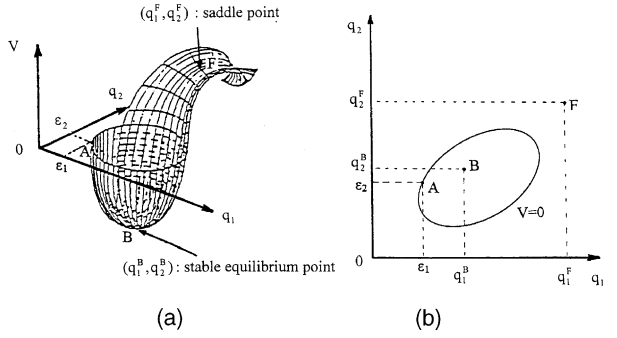


Fig. 2. (a) Energy surface $V$ (at $\lambda^* < \tilde{\lambda}_D$) for a 2-DOF system, and (b) *projection* of motion on $0\,q_1\,q_2$ plane.

The intersection of $V$ with the *horizontal* plane $0\,q_1\,q_2$ is a plane *closed* curve $V = 0$ passing always through the starting point of motion A. Fig. 2b shows the projection of motion in the horizontal plane. If $\lambda < \tilde{\lambda}_D$ any motion starting from A cannot escape via the saddle $F(q_1^F, q_2^F)$ since above the horizontal plane $V > 0$, which implies *no motion* (and hence no dynamic buckling). However, as $\lambda$ increases, the *saddle* F is coming down approaching the horizontal plane $0\,q_1\,q_2$. At $\lambda = \tilde{\lambda}_D$ (for which $V = 0$) the "surface" $V$ *touches* this plane at the saddle D (Fig. 3a). The new closed curve $V = 0$ (intersection of the $V$-surface with the $0\,q_1\,q_2$-plane) passes through the points A and D. The *projection* E′ of the *stable* equilibrium (corresponding to $\tilde{\lambda}_D$) is surrounded by the plane (closed) curve $V = 0$. Since motion occurs only if $V \leqslant 0$, considering the variation of $V(\leqslant 0)$ within the *vertical* plane passing through the equilibria E and D, we observe that $V$ has *minimum* at E and *maximum* at D. A motion that starts from A (taking place in the interior of the surface $V \leqslant 0$) can escape through the *saddle* D only when the points A, E and D are located in the *same vertical* plane (Kounadis, 1996b, 1999). Then, the starting point of motion A coincides with G (Fig. 3b), a fact which implies, $\tilde{\lambda}_D \equiv \lambda_D$. If this is not so (i.e. A $\neq$ G), the motion starting from point A *cannot reach* point D but will stop at a point of the line E′D where the "width" of the curve $V = 0$ (defined by distance between the two points of intersection of $V = 0$ with the normal on E′D) is *smaller* than the "width" of this curve at point A. Then, the motion consists of *back and forth oscillations* between these two points around the *stable* equilibrium E, which is a *centre*. As point A is going *away* from the vertical plane (passing through the points E and D) the difference $E = \lambda_D - \tilde{\lambda}_D$ *increases* (Kounadis, 1996b, 1999). However, by slightly increasing $\lambda$ (above $\tilde{\lambda}_D$) the *closed* curve $V = 0$ becomes an *open* curve exhibiting an "opening" with "width" $\Delta_1\Delta_2$ at the corresponding new saddle D′ (Fig. 4a). If such an "opening" $\Delta_1\Delta_2$ is *smaller* than the width (of the new curve $V = 0$) AA′ at point A (defining the initial amplitude of the

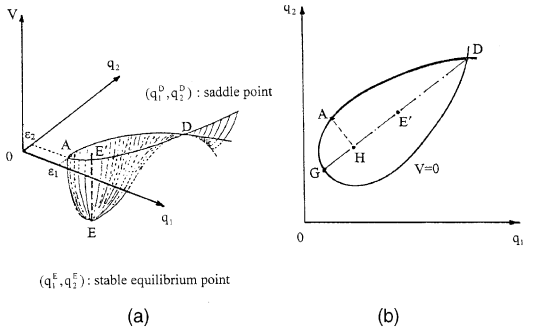


Fig. 3. (a) Total potential surface $V \leqslant 0$ at $\lambda = \tilde{\lambda}_D$, and (b) its intersection with the $0\,q_1\,q_2$ plane for a 2-DOF system.

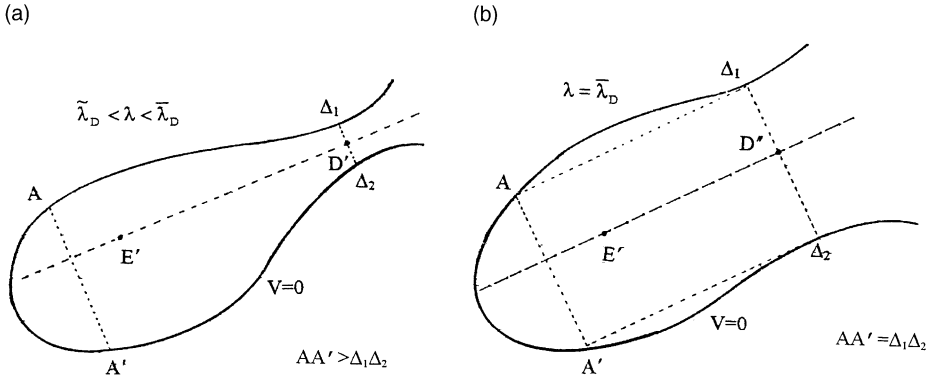


Fig. 4. Curves $V = 0$ for (a) $\tilde{\lambda}_D < \lambda < \bar{\lambda}_D$ and (b) $\lambda = \bar{\lambda}_D$.

motion), an *escaped* motion through the neighbourhood of D′ (where $V(D') < 0$) is *impossible*. Then, we further increase $\lambda$ in such a way so that the "width" of the curve $V = 0$ at A becomes equal to the "width" of this curve at the corresponding *new* saddle D″ (Fig. 4b). Then, an *escaped* motion (and hence dynamic buckling) will occur, and the corresponding to this situation load $\bar{\lambda}_D$ is the DBL. The same approach can be applied to nonconservative systems, using the approximation of $V$ given by Eq. (7).

The *degree of accuracy* of both DBLs $\tilde{\lambda}_D$ and $\bar{\lambda}_D$ depends *basically* on the shape of the closed curve $V = 0$, and more specifically on the *ratio* of the *maximum* "width" versus the *length* of the longitudinal axis DG (Fig. 3b). As this ratio decreases the degree of accuracy of $\tilde{\lambda}_D$ and $\bar{\lambda}_D$ increases appreciably. Moreover, for a given value of this ratio (i.e. for a given shape of the closed curve $V = 0$) the *error* in $\tilde{\lambda}_D$ depends on the *location* of the starting point of motion A relatively to the two points E′ (projection of the stable equilibrium point in the horizontal plane) and the saddle D (Kounadis, 1996b, 1998, 1999). This is quantitatively measured with the aid of the ratio $r = (AH)/(DG)$. The *decrease* of $r$ implies a *much smaller error* in $\tilde{\lambda}_D$. A better estimate of $\tilde{\lambda}_D$ leads to a much more accurate $\bar{\lambda}_D$.

It is worth noticing that for flexurally vibrating systems in their own place (planar systems) the aforementioned ratio of the maximum "width" versus the length (GD) is usually very small (e.g. $<0.20$), a fact that implies a good approximate DBL $\tilde{\lambda}_D$ which subsequently leads to a DBL $\bar{\lambda}_D$ approaching $\lambda_D$ (i.e. $\bar{\lambda}_D \to \lambda_D$). This allows us to consider $\bar{\lambda}_D$ practically as the "exact" DBL for nonconservativeness parameter $\eta$ near 1 (potential system).

The analysis that follows is based on the last *assumption* regarding the shape of the closed curve $V = 0$ (associated with values of the last ratio smaller than 0.20).

## 4. Application to cantilever models

Consider as an example the cantilever model shown in Fig. 5 under (step) partial follower load at its tip. The undeformed state is defined by the initial angles (imperfections) $q_i^0 = \varepsilon_i$ $(i = 1, 2)$ and the deformed state by the generalized coordinates $q_i = \theta_i$ and $\dot{q}_i = \dot{\theta}_i$ $(i = 1, 2)$. As was shown above on the basis of the total energy equation, throughout the motion (including dynamic buckling) $V \leqslant 0$. This quantity for fixed $\lambda$ $(<\lambda_D)$ represents a "surface" in the $V$-displacement space (Fig. 6). The motion takes place in the interior of this "surface", below the horizontal plane $(V \leqslant 0)$. The lowest point of the surface is the stable equilibrium point E*, while the saddle D* gives maximum in $V$ in a certain direction on the stable fundamental path. At $\lambda = \tilde{\lambda}_D$ the intersection of the potential surface $V$ with the horizontal plane gives a level curve $V = 0$ passing through the saddle D. The starting point of motion is located at point A of the curve $V = 0$, whose position

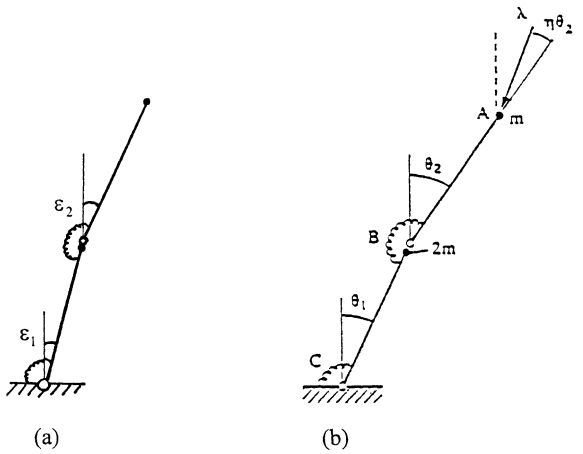


Fig. 5. Two degree-of-freedom cantilever model under partial follower step load.

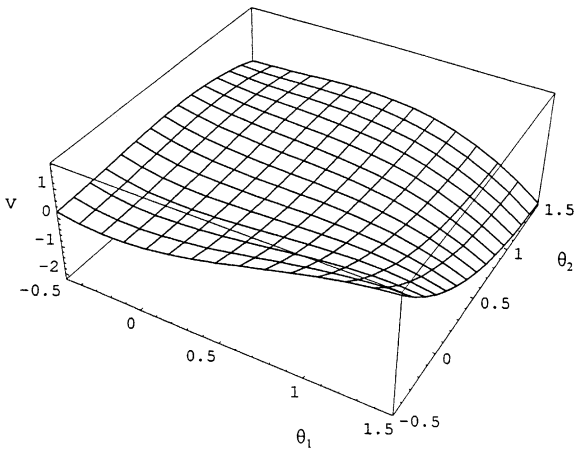


Fig. 6. Perspective view of the energy surface for the 2-DOF model.

depends on the initial conditions $q_i^0 = \varepsilon_1$ and $q_2^0 = \varepsilon_2$. The locations of these points on the static equilibrium path and the contour plot $V = 0$ are shown in Figs. 7 and 8, respectively.

Subsequently, one can visualize the system's motion by the motion of a rigid ball falling under a certain direction without friction and restricted to lie on the interior of the surface $V \leqslant 0$. Let F be the intersection of the curve $V = 0$ with vertical plane passing through the (stable and unstable) equilibria E and D (Fig. 8). If the starting point of motion A coincides with point F, then the ball which suddenly falls from the point F (with $V = 0$) inside the valley of $V < 0$ passes through (or near) the equilibrium point E (with the minimum $V$) and thereafter reaches the saddle D (with $V = 0$). This is so, since the kinetic energy acquired at the stable equilibrium point E is just the right amount to enable the ball to reach the saddle point D. Thus, the ball follows the concrete (unique) trajectory lying on the above vertical plane from point F to the saddle D through which it escapes (dynamic buckling).

For $\eta = 1$ (potential system) it was shown under the above conditions that $\tilde{\lambda}_D \equiv \lambda_D$ (Kounadis, 1996b, 1999); this result holds also in case the starting point of motion A is close to F. As A moves away from F the

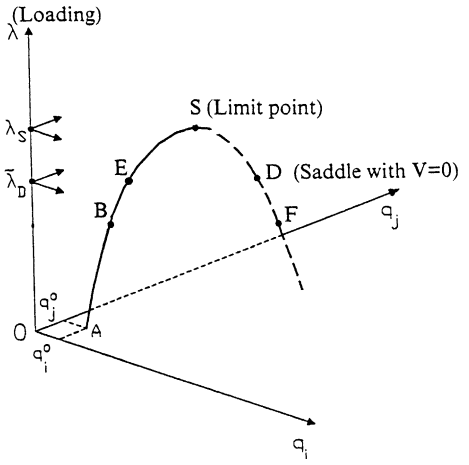


Fig. 7. Static equilibrium path with characteristic points A, E and D.

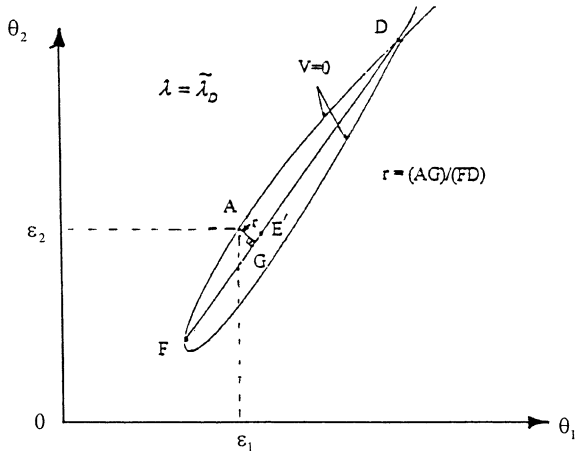


Fig. 8. Contour plot $V = 0$ on the $\theta_1$–$\theta_2$ plane with characteristic points A, E and D.

difference between $\lambda_D$ and $\tilde{\lambda}_D$ increases. Under these circumstances the ball, in general, will not pass through E (with the minimum $V$) but will follow an oscillatory motion whose projection in the horizontal plane $V = 0$ intersects the line E′D between the two portions of the curve $V = 0$ (into which it is divided by E′D) where E′ is the projection of E on the $V = 0$ plane. The amplitudes of oscillations increase as point A goes away from point F. If the projection of the amplitude of motion at A (on the $V = 0$ plane) is less than the opening of the curve $V = 0$ at the saddle D, the ball is directed towards D but does not reach it, and then it returns into the valley undergoing back and forth oscillations. In case the projection of the amplitude of motion at A is equal to the opening of the curve $V = 0$ at D, then the ball escapes through the neighbourhood of the saddle D. Two typical plots of the projection of motion on the horizontal plane $0\theta_1\theta_2$ are shown in Fig. 9a and b, one for stable motion and one for unstable motion.

From a large number of numerical results for both quadratic and cubic conservative models it was established that the relative error $(\lambda_D - \tilde{\lambda}_D)/\lambda_D$ increases as the distance $r = AG/FD$ (Fig. 8) of the point A from the vertical plane (divided by the distance FD) increases. Given that the projection G of the starting

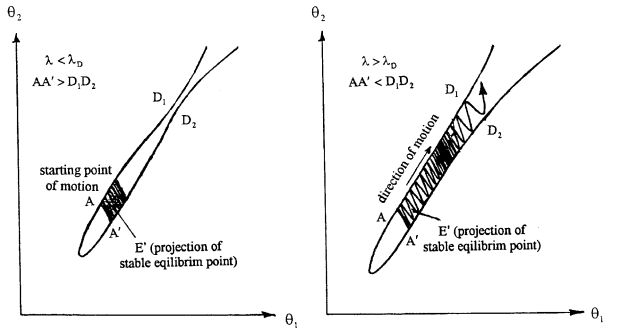


Fig. 9. Contour plots $V = 0$ and projection of motion for stable and unstable motions.

point of motion A on the straight line DE′, cannot be between E′ and D, the maximum error of $\tilde{\lambda}_D$ occurs when point G tends to coincide with E′. However, even in this case, the error in $\tilde{\lambda}_D$ lies usually within the bounds of the engineering accuracy (i.e. not greater than 10%).

For $\eta \neq 1$ (nonpotential) systems the above result was verified qualitatively, even though the curve $(\lambda_D - \tilde{\lambda}_D)/\lambda_D$ vs $r$ was found to depend on $\eta$. This is so because the value of $\eta$ defines the *initial* direction of the motion from the starting point A. The corresponding load $\tilde{\lambda}_D$ is an approximate DBL (associated with vanishing but nonzero damping) which may be either greater or smaller than $\lambda_D$, while for $\eta = 1$ always $\tilde{\lambda}_D < \lambda_D$. Hence, for nonpotential systems $\tilde{\lambda}_D$ is not a lower bound of $\lambda_D$ as in case of potential systems (Kounadis, 1996b, 1999).

Then, the approximate DBLs $\overline{\lambda}_D$ were obtained for values of $\eta$ equal to 0.6, 0.7, 0.8 and 0.9. The computational effort required to compute $\overline{\lambda}_D$ is much higher than for $\tilde{\lambda}_D$. This is worthwhile for systems that are not highly nonconservative (values of $\eta$ near to 1), since for such systems $\overline{\lambda}_D$ is considerably more accurate than $\tilde{\lambda}_D$. For values of $\eta$ equal to 0.6 or 0.7 this is not the case and the $\overline{\lambda}_D$ approximation is not better than the $\tilde{\lambda}_D$ approximation (Kounadis and Gantes, 2000). However, $\overline{\lambda}_D$ is in most cases an upper bound of the exact DBL and $\tilde{\lambda}_D$ a lower bound, which is a very useful conclusion for practical purposes. Furthermore, the average of $\overline{\lambda}_D$ and $\tilde{\lambda}_D$ is a very good estimate of DBL, usually better than $\overline{\lambda}_D$ and $\tilde{\lambda}_D$.

## 5. Numerical results

The theory and findings of this study will be illustrated via several analyses of the 2-DOF model shown in Fig. 5 for which a lot of numerical results have been obtained for several values of $\eta$. This model is governed by the following dimensionless equations of motion (Kounadis, 1994; Kounadis et al., 1992).

$$\begin{aligned}&(1+m)\ddot{\theta}_1 + \ddot{\theta}_2\cos(\theta_1-\theta_2) + \dot{\theta}_2^2\sin(\theta_1-\theta_2) + \left(c_1^* + c_2^*\right)\dot{\theta}_1 - c_2^*\dot{\theta}_2 + V_1 = 0\\ &\ddot{\theta}_2 + \ddot{\theta}_1\cos(\theta_1-\theta_2) - \dot{\theta}_1^2\sin(\theta_1-\theta_2) + c_2^*\dot{\theta}_2 - c_2^*\dot{\theta}_1 + V_2 = 0\end{aligned} \tag{9}$$

where $m = m_1/m_2$, $c_i^*$ $(i = 1, 2)$ are damping coefficients and

$$\begin{aligned}V_1 = {} & \theta_1 - \varepsilon_1 + \delta_1(\theta_1-\varepsilon_1)^2 + \gamma_1(\theta_1-\varepsilon_1)^3 - (\theta_2-\varepsilon_2-\theta_1+\varepsilon_1) - \delta_2(\theta_2-\varepsilon_2-\theta_1+\varepsilon_1)^2 - \gamma_2(\theta_2-\varepsilon_2\\ & -\theta_1+\varepsilon_1)^3 - \lambda\sin[\theta_1 + (\eta-1)\theta_2]\end{aligned}$$

$$V_2 = \theta_2 - \varepsilon_2 - \theta_1 + \varepsilon_1 + \delta_2(\theta_2-\varepsilon_2-\theta_1+\varepsilon_1)^2 - \gamma_2(\theta_2-\varepsilon_2-\theta_1+\varepsilon_1)^3 - \lambda\sin\eta\theta_2 \tag{10}$$

$V_1 = V_2 = 0$ are the equilibrium equations.

Multiplying the 1st and 2nd of Eq. (9) by $\dot{\theta}_1$ and $\dot{\theta}_2$ respectively, integrating with respect to time and summing up the resulting equations, we obtain, for the system initially $(t = 0)$ unstressed, the following energy-balance equation

$$K + U + 2\int_0^\tau F\,\mathrm{d}\tau' - \lambda\left\{\int_0^\tau \sin[\theta_1 + (\eta-1)\theta_2]\dot{\theta}_1\,\mathrm{d}\tau' + \int_0^\tau \sin\eta\theta_2 \cdot \dot{\theta}_2\,\mathrm{d}\tau'\right\} = 0 \tag{11}$$

where

$$\begin{aligned} K &= \tfrac{1}{2}(1+m)\dot{\theta}_1^2 + \tfrac{1}{2}[\dot{\theta}_2^2 + 2\dot{\theta}_1\dot{\theta}_2\cos(\theta_1-\theta_2)] \\ U &= \tfrac{1}{2}(\theta_1-\varepsilon_1)^2 + \tfrac{1}{3}\delta_1(\theta_1-\varepsilon_1)^3 + \tfrac{1}{4}\gamma_1(\theta_1-\varepsilon_1)^4 + \tfrac{1}{2}(\theta_2-\varepsilon_1-\theta_1+\varepsilon_1)^2\tfrac{1}{3}\delta_2(\theta_2-\varepsilon_1-\theta_1+\varepsilon_1)^3 + \\ &\quad + \tfrac{1}{4}\gamma_2(\theta_2-\varepsilon_1-\theta_1+\varepsilon_1)^4 \\ F &= \tfrac{1}{2}c_1^*\dot{\theta}_1^2 + \tfrac{1}{2}c_2^*(\dot{\theta}_2-\dot{\theta}_1)^2 \end{aligned} \tag{12}$$

The equivalent expression of $V$ in Eq. (7), due to relation (11), is given by

$$V = U - \lambda\left\{\int_0^\tau \sin[\theta_1 + (\eta-1)\theta_2]\dot{\theta}_1\,\mathrm{d}\tau' + \int_0^\tau \sin\eta\theta_2 \cdot \dot{\theta}_2\,\mathrm{d}\tau'\right\} \tag{13}$$

The first of these two integrals is not integrable in terms of known functions, but the function $\sin[\theta_1 + (\eta-1)\theta_2]$ is monotone for very small values of $\theta_i$ $(i = 1, 2)$. In this case, using the mean-value theorem for integrals, one can adopt the following approximation:

$$\int_0^\tau \sin[\theta_1 + (\eta-1)\theta_2]\dot{\theta}_1\,\mathrm{d}\tau' \cong (\theta_1-\varepsilon)\sin\left[\theta_1^{av} + (\eta-1)\theta_2^{av}\right] \tag{14}$$

Another approximation which can also be adopted using the above theorem is

$$\begin{aligned} \int_0^\tau \sin[\theta_1 + (\eta-1)\theta_2]\dot{\theta}_1\,\mathrm{d}\tau' &\cong \cos[\varepsilon_1 + (\eta-1)\varepsilon_2] - \cos[\theta_1 + (\eta-1)\theta_2] + (1-\eta)(\theta_2-\varepsilon_2) \\ &\times \sin\left[\theta_1^{av} + (\eta-1)\theta_2^{av}\right] \end{aligned} \tag{15}$$

where $\theta_1^{av} = (\theta_1 + \varepsilon_1)/2$ and $\theta_2^{av} = (\theta_2 + \varepsilon_2)/2$ are the average values of the corresponding angles.

Taking the mean value of approximations (14) and (15), the expression of $V$ in Eq. (13) becomes

$$\begin{aligned} V \cong U - \frac{\lambda}{2}\Bigg\{&(\theta_1-\varepsilon)\sin\left[\theta_1^{av} + (\eta-1)\theta_2^{av}\right] + \cos[\varepsilon_1 + (\eta-1)\varepsilon_2] - \cos[\theta_1 + (\eta-1)\theta_2] + (1-\eta) \\ &\times (\theta_2-\varepsilon_2)\sin\left[\theta_1^{av} + (\eta-1)\theta_2^{av}\right] - \frac{2}{\eta}[\cos\eta\theta_2 - \cos\eta\varepsilon_2]\Bigg\} \end{aligned} \tag{16}$$

Using this expression for the case of vanishing but nonzero damping $(c_{ij} \to 0$ for $i, j = 1, 2)$ we obtain the approximate values $\tilde{\lambda}_\mathrm{D}$, $\tilde{\theta}_1^\mathrm{D}$ and $\tilde{\theta}_2^\mathrm{D}$ without solving the nonlinear initial-value problem. For this model it was found that for given $\eta$ the ratio $(\lambda_\mathrm{D} - \tilde{\lambda}_\mathrm{D})/\lambda_\mathrm{D}$ representing the relative error of $\tilde{\lambda}_\mathrm{D}$ is a nonlinear function of the length ratio $r = \mathrm{AG}/\mathrm{FD}$ (see Fig. 8). The error estimates have been obtained by comparison to numerical results making use of the Runge-Kutta scheme. From Fig. 10 one can see the relation $E = (\lambda_\mathrm{D} - \tilde{\lambda}_\mathrm{D})/\lambda_\mathrm{D}$ vs $r$ corresponding to $\eta = 0.60$, 0.70, 0.80 and 0.90. Clearly, as $r$ increases the error $E$ (%) also increases. Figs. 11–14 show the error distribution $E$ (%) of both $\overline{\lambda}_\mathrm{D}$ and $\tilde{\lambda}_\mathrm{D}$. It is clear that as $\eta$ decreases the difference of $\overline{\lambda}_\mathrm{D}$ and $\tilde{\lambda}_\mathrm{D}$ increases. For $\eta < 0.50$ the proposed procedure becomes inapplicable because the model loses its stability by flutter instead of divergence (Kounadis et al., 1992).

It is worth noticing that these plots are based on a 2-DOF model with uniform mass distribution. However, even in the extreme case that one of the masses of the model is 100 times larger than the other,

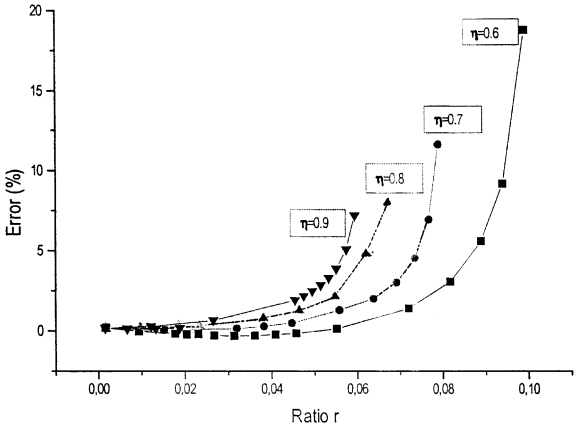


Fig. 10. Correlation between $r$ and the error of the approximate buckling load.

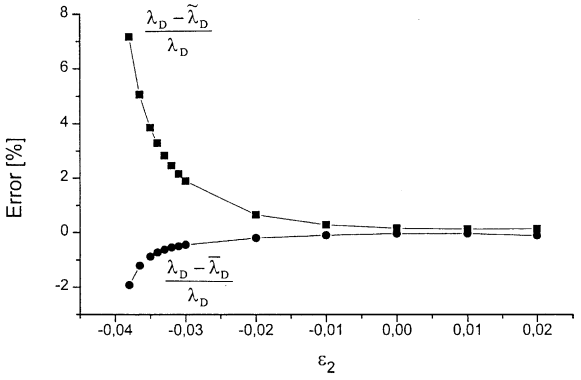


Fig. 11. Error distributions of $\bar{\lambda}_D$ and $\tilde{\lambda}_D$ for $\eta = 0.90$.

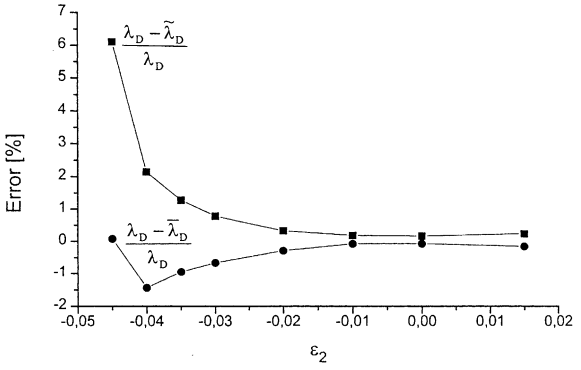


Fig. 12. Error distributions of $\bar{\lambda}_D$ and $\tilde{\lambda}_D$ for $\eta = 0.80$.

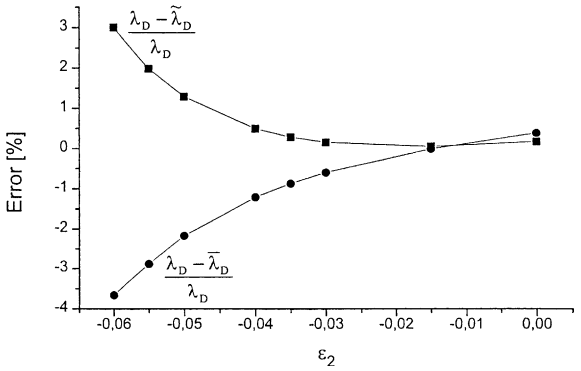


Fig. 13. Error distributions of $\bar{\lambda}_D$ and $\tilde{\lambda}_D$ for $\eta = 0.70$.

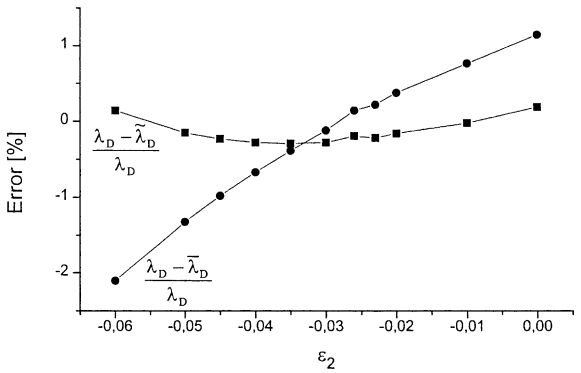


Fig. 14. Error distributions of $\bar{\lambda}_D$ and $\tilde{\lambda}_D$ for $\eta = 0.60$.

this effect on the DBL is less than 1.4%. Hence, $\lambda_D$ is practically independent of the mass distribution. This phenomenon was originally observed in imperfection sensitive conservative systems (Kounadis, 1999).

The results of Figs. 10–14 refer to a model with $\delta_1 = -2.50$, $\delta_2 = -0.75$, $\gamma_1 = \gamma_2 = 0$, $m = 2$, $c_1 \to 0$, $c_2 \to 0$, $\varepsilon_1 = 0.05$. For the case $\eta = 0.8$ the numerical results are also presented in tabular form in Table 1.

The appreciably increased accuracy of the improved approximation $\bar{\lambda}_D$ with respect to the initial approximation $\tilde{\lambda}_D$ is evident.

Table 1
Numerical values of ratio $r$ and approximate dynamic loads $\tilde{\lambda}_D$ and $\bar{\lambda}_D$ and their accuracy compared to exact load $\lambda_D$ for a system with $\eta = 0.8$, $\delta_1 = -2.50$, $\delta_2 = -0.75$, $\gamma_1 = \gamma_2 = 0$, $m = 2$, $c_1 \to 0$, $c_2 \to 0$, $\varepsilon_1 = 0.05$ and various values of $\varepsilon_2$

| $\varepsilon_2$ | $\lambda_D$ | $\tilde{\lambda}_D$ | $r$ | $((\lambda_D - \tilde{\lambda}_D)/\lambda_D)100$ (%) | $\bar{\lambda}_D$ | $((\lambda_D - \tilde{\lambda}_D)/\lambda_D)100$ (%) |
|---|---|---|---|---|---|---|
| −0.045 | 0.419960 | 0.394309 | 0.062016 | 6.108 | 0.419623 | 0.080 |
| −0.04 | 0.388766 | 0.380425 | 0.054705 | 2.146 | 0.394369 | −1.441 |
| −0.035 | 0.372629 | 0.367877 | 0.046423 | 1.275 | 0.376161 | −0.948 |
| −0.03 | 0.359333 | 0.356516 | 0.038129 | 0.784 | 0.361721 | −0.665 |
| −0.02 | 0.337861 | 0.336752 | 0.02328 | 0.328 | 0.338836 | −0.289 |
| −0.01 | 0.320660 | 0.320072 | 0.011273 | 0.183 | 0.320885 | −0.070 |
| 0 | 0.306215 | 0.305707 | 0.001631 | 0.166 | 0.305998 | −0.071 |
| 0.015 | 0.288062 | 0.287374 | 0.009686 | 0.239 | 0.287618 | −0.0154 |

It should be noted that the proposed approach can be extended to $n$-DOF systems. For such systems, for fixed $\lambda$, $V$ represents a "hypersurface" in the $(n+1)$-dimensional space spanned by $V$ and $q_i$ $(i = 1, \ldots, n)$. A series of hypersurfaces correspond to different, constant values of $\lambda$. For 2-DOF systems these hypersurfaces are geometric surfaces, which are much easier to visualize. For this reason, 2-DOF systems have been selected to demonstrate this concept. However, the analytical and numerical calculations associated with this approach can be easily extended to complex systems with more DOF. Actually, for such systems the results are not only going to be more useful due to the increased difficulty of obtaining numerical solutions, but are also expected to be more accurate due to the stricter restrictions imposed upon the motion by the higher number of DOF.

## 6. Conclusions

The most important conclusions are the following:

1. The limit point load obtained via a *static* stability analysis does not represent the actual critical load of imperfection sensitive systems. This can be determined by using a nonlinear dynamic analysis which yields always a lower critical load than the limit point load. The difference between the static and dynamic critical load reveals the dynamic character of the follower loading.

2. Despite the lack of a potential for systems under follower loading, useful criteria for dynamic buckling based on an energy-balance equation similar to those valid for potential (conservative) systems were established.

3. These energy-criteria together with geometrical considerations of the motion channel allow us to predict a priori for a 2-DOF nondissipative model the accuracy of the DBL $\tilde{\lambda}_D$. More specifically, the smaller the distance of the starting point of motion from the straight line connecting the stable and unstable equilibria corresponding to $\tilde{\lambda}_D$, the more accurate $\tilde{\lambda}_D$. Contrary to potential systems where $\tilde{\lambda}_D$ is always a lower bound of the exact DBL $\lambda_D$, for nonpotential systems $\tilde{\lambda}_D$ may be greater or smaller than $\lambda_D$.

4. Further energy considerations allow us to establish another approximate load $\overline{\lambda}_D$ of the exact DBL, very good for $\eta$ near 1. For the cases examined, $\overline{\lambda}_D$ is practically a lower bound of the exact DBL and $\tilde{\lambda}_D$ an upper bound, which is a very useful conclusion for practical purposes. The average of $\overline{\lambda}_D$ and $\tilde{\lambda}_D$ can also be used as a DBL.

5. The proposed methodology can be extended to N-DOF nonpotential systems.

## Acknowledgements

This work has been partially financed by INTAS, the International Association for the promotion of cooperation with scientists from the New Independent States of the former Soviet Union. This support is gratefully acknowledged.

## References

Bolotin, V.V., 1963. Nonconservative Problems of the Theory of Elastic Stability, Pergamon Press, New York.

Huseyin, K., 1978. Vibration and Stability of Multiple-Parameter Systems, Sijthoff and Noordhoff, The Netherlands.

Inman, D.J., 1983. Dynamics of asymmetric nonconservative systems. J. Appl. Mech. ASME 50, 199–203.

Kandakis, G., Kounadis, A.N., 1992. On the large postbuckling response of nonconservative continuous systems. Arch. Appl. Mech. 62, 256–265.

Kounadis, A.N., 1977. Stability of elastically restrained Timoshenko cantilevers with attached masses subjected to follower forces. J. Appl. Mech. ASME 44, 731–736.

Kounadis, A.N., 1983. The existence of regions of divergence instability for nonconservative systems under follower loads. Int. J. Solids Struct. 9, 725–733.

Kounadis, A.N., 1991. On the reliability of postbuckling analyses for nonconservative imperfect systems. Arch. Mech. (Warsaw) 43, 95–105.

Kounadis, A.N., 1992. On the paradox of the destabilizing effect of damping in nonconservative systems. Int. J. Non-Linear Mech. 27 (4), 597–609.

Kounadis, A.N., 1994a. On the failure of static stability analyses of nonconservative systems in regions of divergence instability. Int. J. Solids Struct. 31 (15), 2099–2120.

Kounadis, A.N., 1994b. A Qualitative analysis for the local and global dynamic buckling and stability of autonomous discrete systems. Quart. J. Mech. Appl. Math. 47 (2), 269–295.

Kounadis, A.N., 1995. Nonlinear stability and dynamic buckling of autonomous dissipative systems. Z. Angew. Math. Mech. 75 (4), 283–293.

Kounadis, A.N., 1996a. Non-linear dynamic buckling of a simple model via Liapunov direct method. J. Sound Vibr. 193 (5), 1091–1097.

Kounadis, A.N., 1996b. On the nonlinear dynamic buckling mechanism of autonomous dissipative/nondissipative discrete structural systems. Arch. Appl. Mech. 66, 395–408.

Kounadis, A.N., 1998. Qualitative criteria for dynamic buckling of imperfection sensitive non-conservative systems. Int. J. Mech. Sci. 40 (10), 949–962.

Kounadis, A.N., 1999. A geometric approach for establishing dynamic buckling loads of autonomous potential two-degree-of-freedom systems. J. Appl. Mech. 66, 55–61.

Kounadis, A.N., Simitses, G.J., 1993. Local classical and global bifurcations in non-linear, non-gradient autonomous dissipative structural systems. J. Sound Vibr. 160 (3), 417–432.

Kounadis, A.N., Simitses, G.J., 1997. Nonconservative systems with symmetrizable stiffness matrices exhibiting limit cycles. Int. J. Non-Linear Mech. 32 (3), 515–529.

Kounadis, A.N., Gantes, C.J., 2000. Approximate Dynamic Buckling Loads of Nonconservative Structural Systems via Energy Considerations, 20th International Congress of Theoretical and Applied Mechanics (ICTAM 2000), Chicago, 27 August–2 September 2000.

Kounadis, A.N., Avraam, T., Mallis, J., 1992. On the reliability of classical divergence instability analyses of Ziegler's nonconservative model. Comp. Math. Appl. Mech. Engng. 95, 317–330.

Leipholz, H., 1970. Stability Theory, an Introduction to the Stability of Dynamic Systems and Rigid Bodies, Academic Press, New York.

Moran, T.J., 1970. A simple alternative to the Routh–Hurwitz criterion for symmetric systems. J. Appl. Mech. 37, 1168–1170.

Paidoussis, M.P., 1997. Fluid-Structure Interactions: Slender Bodies and Axial Flow, Academic Press, London.

Plaut, R.H., 1976. Postbuckling analysis of nonconservative elastic systems. J. Struct. Mech. 4 (4), 395–416.

Walker J.A, Schmitendorf, W.E., 1973. A simple test for asymptotic stability in partially dissipative symmetric systems. J. Appl. Mech. 40, 1120–1121.

Ziegler, H., 1952. Die Stabilitatskriterien der Elastomechanik. Ingenieur-Archiv 20, 49–52.